

3D marine Controlled-Source Electromagnetic Interferometry by multidimensional deconvolution in the wavenumber domain for a sparse receiver grid

Jürg Hunziker, Evert Slob, Yuanzhong Fan, Roel Snieder and Kees Wapenaar

summary

We use interferometry by multidimensional deconvolution in combination with synthetic aperture sources in 3D to suppress the airwave and the direct field, and to decrease source uncertainty in marine Controlled-Source electromagnetics. We show that the method works for very large receiver spacing distances, even though the thereby retrieved reflection response may be aliased.

Introduction

With interferometry by multidimensional deconvolution (MDD), the medium above the receivers is replaced by a homogeneous halfspace of the same material as at the receiver level. Furthermore, the direct field is suppressed and the sources are redatumed to receiver locations. Consequently, with interferometry by MDD, we retrieve the subsurface reflection response or, in other words, the scattered Green's function of the subsurface. Since interferometry is a data-driven method, no information about the medium or about the source location are required. Only the medium parameters at the receiver level as well as the location and orientation of the receivers are necessary. More information about interferometry by MDD for Controlled-Source Electromagnetics (CSEM) is given by Wapenaar et al. (2008) and Hunziker et al. (2012). The benefits of marine CSEM-interferometry are as follows: (1) the subsurface signal is extracted and (2) source uncertainty is reduced. Therefore, we assume that using the reflection response instead of common CSEM data as an input for a scheme that inverts for the subsurface conductivity distribution leads to a more precise image of the subsurface.

Method

Interferometry by MDD requires properly sampled data, i.e., dense enough for a large enough offset range without gaps. Since standard CSEM data is sampled rather sparse, the first step of our processing scheme is to apply the synthetic-aperture-source concept (Fan et al., 2010) in order to filter out high wavenumbers. These high wavenumbers correspond to the direct field or reflections from shallow interfaces. Thereby, the signal from a potential hydrocarbon reservoir is not altered, because that signal features low wavenumbers due to the typically great depth of reservoirs.

In the second step of the interferometry processing scheme, the electromagnetic field is split into an upward decaying transverse-magnetic (TM) component $P^{TM,-}$, an upward decaying transverse-electric (TE) mode component $P^{TE,-}$ and the two corresponding downward decaying TM- and TE-mode components $P^{TM,+}$ and $P^{TE,+}$. The algorithm used here (Slob, 2009) requires the four horizontal components of the electromagnetic field as well as the material parameters at the receiver level. After decomposition, the upward decaying field can be related to the downward decaying field via the reflection response R , including data from an inline oriented source (x-src) and a crossline oriented source (y-src):

$$\begin{pmatrix} \tilde{P}_{x\text{-src}}^{TM,-} & \tilde{P}_{y\text{-src}}^{TM,-} \\ \tilde{P}_{x\text{-src}}^{TE,-} & \tilde{P}_{y\text{-src}}^{TE,-} \end{pmatrix} = \begin{pmatrix} \tilde{R}^{TM,TM} & \tilde{R}^{TM,TE} \\ \tilde{R}^{TE,TM} & \tilde{R}^{TE,TE} \end{pmatrix} \begin{pmatrix} \tilde{P}_{x\text{-src}}^{TM,+} & \tilde{P}_{y\text{-src}}^{TM,+} \\ \tilde{P}_{x\text{-src}}^{TE,+} & \tilde{P}_{y\text{-src}}^{TE,+} \end{pmatrix}, \quad (1)$$

where the tilde denotes the frequency-wavenumber domain. The reflection response features two superscripts indicating TM- or TE-mode. The reason is that besides pure TM-mode and pure TE-mode reflection responses also mode conversions are possible in a medium that contains lateral variations.

In the third and final step of the interferometry processing flow, we solve equation 1 for the matrix of reflection responses using a multidimensional deconvolution. This can be done efficiently in the frequency-wavenumber domain for each wavenumber separately assuming a laterally invariant medium:

$$\begin{pmatrix} \tilde{R}^{TM,TM} & \tilde{R}^{TM,TE} \\ \tilde{R}^{TE,TM} & \tilde{R}^{TE,TE} \end{pmatrix} = \begin{pmatrix} \tilde{P}_{x\text{-src}}^{TM,-} & \tilde{P}_{y\text{-src}}^{TM,-} \\ \tilde{P}_{x\text{-src}}^{TE,-} & \tilde{P}_{y\text{-src}}^{TE,-} \end{pmatrix} \left[\begin{pmatrix} \tilde{P}_{x\text{-src}}^{TM,+} & \tilde{P}_{y\text{-src}}^{TM,+} \\ \tilde{P}_{x\text{-src}}^{TE,+} & \tilde{P}_{y\text{-src}}^{TE,+} \end{pmatrix} + \varepsilon^2 \begin{pmatrix} 1 & 0 \\ 0 & 1 \end{pmatrix} \right]^{-1}, \quad (2)$$

where ε is a stabilization parameter. Non-zero $\tilde{R}^{TM,TE}$ and $\tilde{R}^{TE,TM}$ indicate lateral variations of the medium, requiring the usage of a space-domain implementation.

Numerical example

We apply this processing flow to a numerical dataset. A slice of the model, which is a stack of horizontal layers, is depicted in Figure 1. The retrieved reflection response for the pure TM-mode in the wavenumber domain $\tilde{R}^{TM,TM}$ is plotted in Figure 2 for various receiver spacings. Increasing the receiver

spacing in the space domain corresponds to limiting the range of wavenumbers in the wavenumber domain, i.e. decreasing the Nyquist wavenumber. The retrieved reflection responses miss one datapoint at zero wavenumber, because a finite source does not excite that wavenumber component. The gap is filled by assigning the value of a neighboring point to the missing datapoint. The relative error of the retrieved reflection response relative to the directly-modeled bandlimited reflection response (Figure 2) never exceeds 3% except for wavenumbers close to the Nyquist wavenumber. Neglecting those artifacts, the retrieval of the reflection response in the wavenumber domain is considered very good for all receiver spacings. Before the Fourier transform is applied, to get the space-domain result, a taper is used to damp the artifacts at high wavenumbers.

The inverse Fourier transformed reflection responses of Figure 2 are shown in Figure 3. For a receiver spacing of $dx = 160$ m, the reflection response is retrieved perfectly. The relative error between the retrieved and the directly-modeled bandlimited reflection response is smaller than 3% except at large offsets. At those offsets, the amplitude of the reflection response has decayed already over more than four orders of magnitude. Even small errors can lead to large relative errors at so small amplitudes. We therefore neglect those relative errors. A receiver spacing of 320 m introduces small artifacts at zero inline or zero crossline offset. These artifacts are even more pronounced for a receiver spacing of 640 m. They are caused during the Fourier transform because the retrieved reflection response is aliased at that receiver spacing as can be seen in the limited wavenumber range in Figure 2. For a receiver spacing of 1280 m, these artifacts are no longer confined to zero inline or crossline offsets. Therefore, the relative error is increased at all offsets. Still, within the bandwidth defined by the receiver spacing, the retrieval is correct also for the largest receiver spacing (Figure 2g and 2h). Consequently, the method works also for very large receiver spacings or, in other words, for a very limited bandwidth, even if the bandwidth of the data is narrower than the bandwidth of the subsurface response.

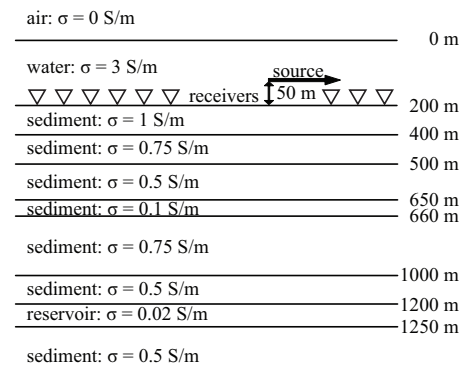


Figure 1 A slice of the model (not to scale). The conductivity σ is given for each layer.

Conclusions

CSEM interferometry by MDD using synthetic aperture sources in 3D is able to retrieve the reflection response properly even for very large receiver spacings. However, the bandwidth of the subsurface reflection response may be broader than the bandwidth of the data, leading to a bandlimited retrieved reflection response. Although the method works for very large receiver spacings, it may be advisable to sample denser in order to avoid aliasing of the subsurface signal.

Acknowledgements

This research is supported by the Dutch Technology Foundation STW, applied science division of NWO and the Technology Program of the Ministry of Economic Affairs (grant DCB.7913).

References

- Fan, Y. et al. [2010] Synthetic aperture controlled source electromagnetics. *Geophys. Res. Lett.*, **37**, L13305.
- Hunziker, J., Slob, E., Fan, Y., Snieder, R. and Wapenaar, K. [2012] Two-dimensional controlled-source electromagnetic interferometry by multidimensional deconvolution: spatial sampling aspects. *Geophysical Prospecting*, **60**, 974–994.
- Slob, E. [2009] Interferometry by Deconvolution of Multicomponent Multioffset GPR Data. *IEEE Transactions on Geoscience and Remote Sensing*, **47**, 828–838.
- Wapenaar, K., Slob, E. and Snieder, R. [2008] Seismic and electromagnetic controlled-source interferometry in dissipative media. *Geophysical Prospecting*, **56**, 419–434.

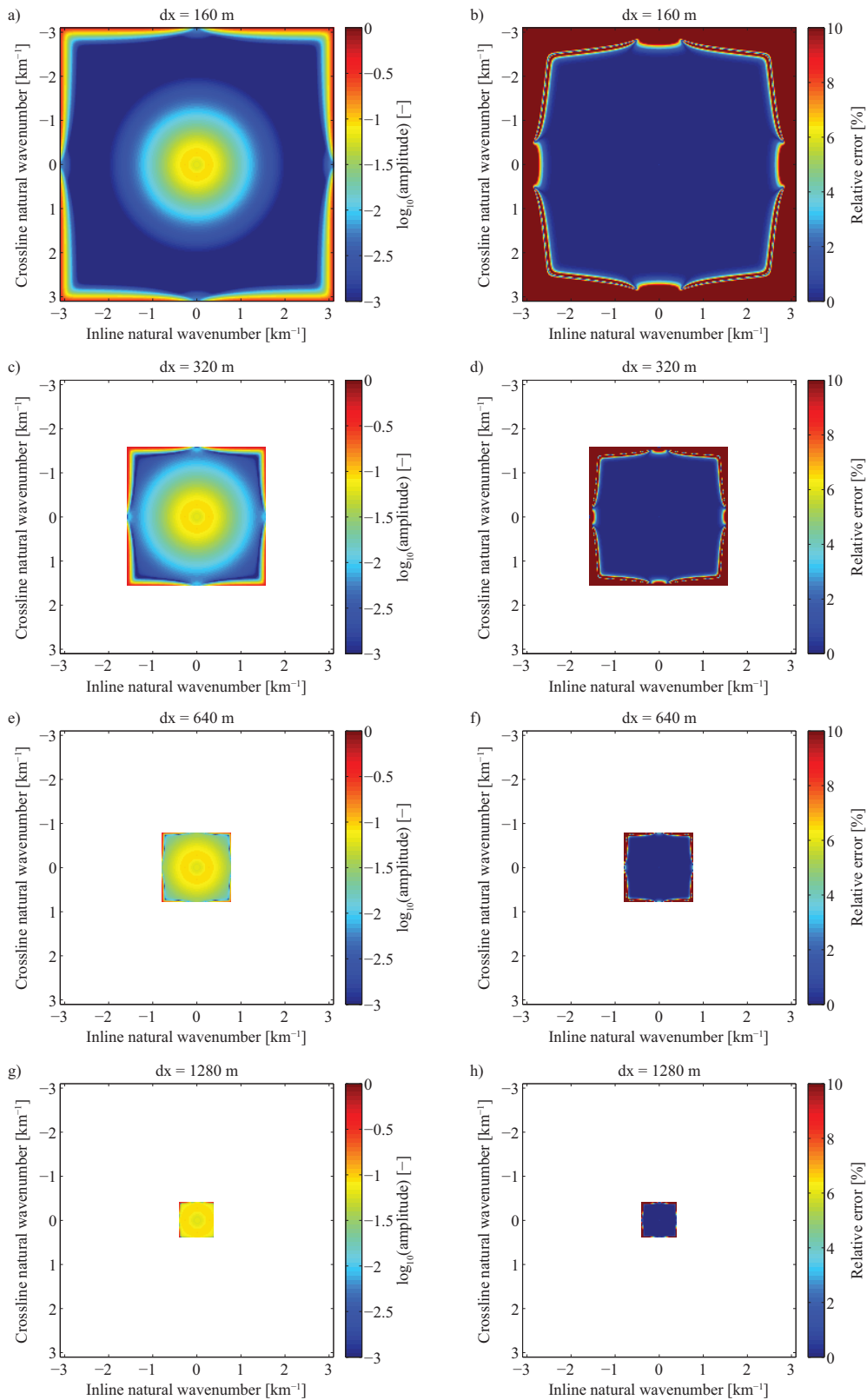


Figure 2 The retrieved reflection response for the pure TM-mode in the wavenumber domain $\tilde{R}^{TM, TM}$ (left column) and the relative error relative to the directly-modeled bandlimited reflection response (right column) for a receiver spacing dx of a) b) 160 m, c) d) 320 m, e) f) 640 m and g) h) 1280 m. Note that the natural wavenumber is defined as the radial wavenumber divided by 2π .

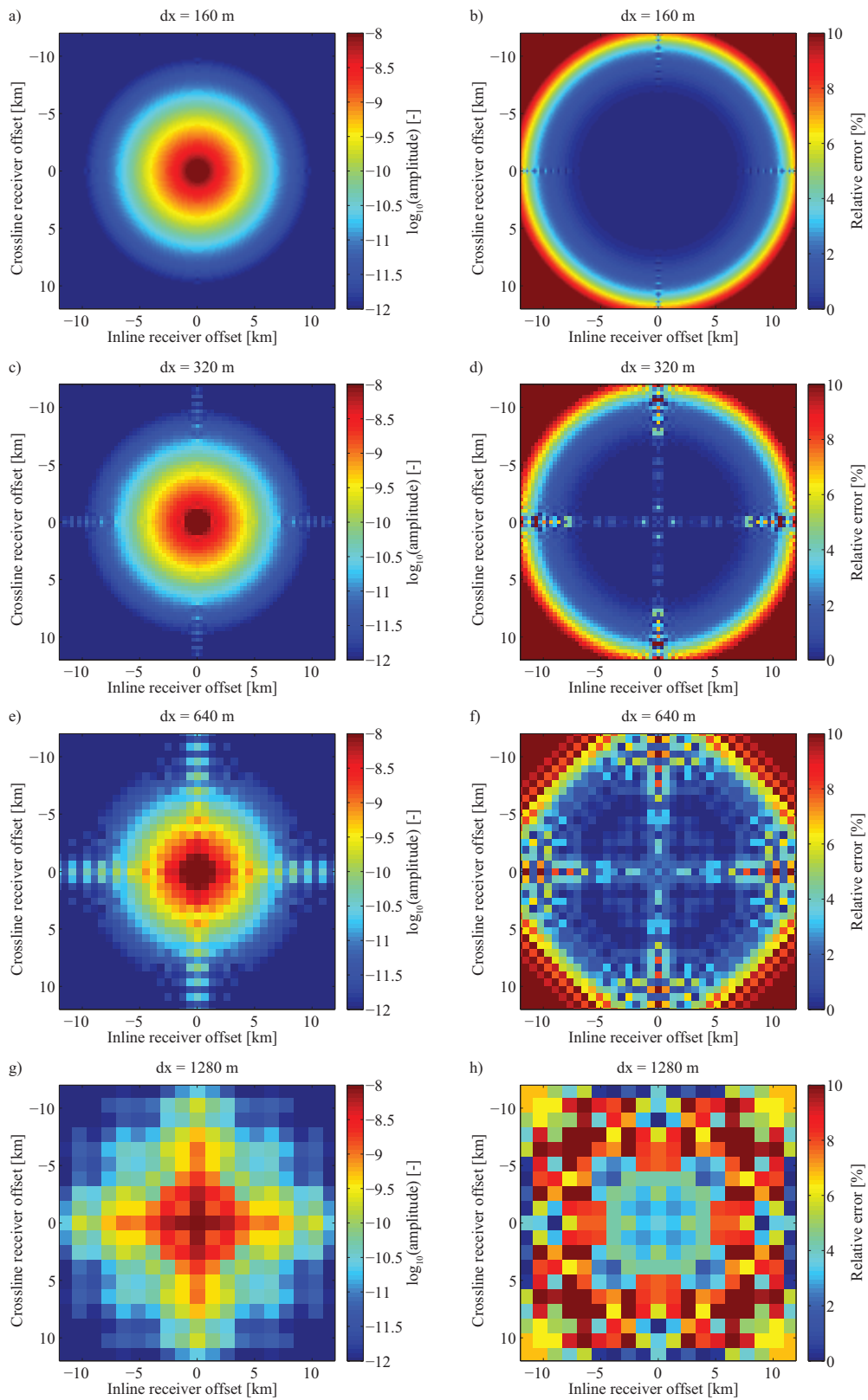


Figure 3 Same as Figure 2 but in the space domain.